

Electronic structures of quasi-one-dimensional ferrimagnetic insulator $\text{Ca}_3\text{Co}_2\text{O}_6$

Tay-Rong Chang^{a,*}, Horng-Tay Jeng^{b,a,*}, Chen-Shiung Hsue^a

^a Department of Physics, National Tsing Hua University, Hsinchu 30013, Taiwan

^b Institute of Physics, Academia Sinica, Taipei 11529, Taiwan

ARTICLE INFO

Article history:

Received 2 March 2010

Received in revised form 22 July 2010

Accepted 5 August 2010

Available online 26 August 2010

Keywords:

First-principles calculations

Orbital ordering

Strong correlation

ABSTRACT

The electronic structures of quasi-one-dimensional ferrimagnetic $\text{Ca}_3\text{Co}_2\text{O}_6$ are investigated using the generalized gradient approximation (GGA) as well as the GGA plus on-site Coulomb interaction (GGA + U) scheme. GGA + U calculations reveal that the interchain ferrimagnetic $\text{Ca}_3\text{Co}_2\text{O}_6$ is a Mott–Hubbard insulator rather than a metal given from GGA. In addition, we found an on-site U induced $3z^2 - r^2$ orbital ordering on Co_{pri} sublattice which drives the intrachain ferromagnetic coupling along c -axis. Our findings suggest that strong electron–electron correlation plays an important role in $\text{Ca}_3\text{Co}_2\text{O}_6$.

Crown Copyright © 2010 Published by Elsevier B.V. All rights reserved.

1. Introduction

The quasi-one-dimensional ferrimagnetic insulator $\text{Ca}_3\text{Co}_2\text{O}_6$ has attracted considerable attention in recent years due to the stair-step jumps in the magnetization under applied magnetic field [1–7]. At $H = 5$ T (along c -axis), the magnetic moments align ferromagnetically (FM) with a saturation magnetization (M_s) of $\sim 4.8\mu_B$ [1–5]. A rapid transition from the FM state into the ferrimagnetic state with a plateau magnetization of about $M_s/3$ is observed at $H_c \approx 3.6$ T [1–7]. Below ~ 3.6 T (with temperature less than 10 K), the $M(H)$ curve becomes strongly hysteretic and exhibits several additional magnetization steps at $H = 1.2, 2.4,$ and 3.6 T [2–7]. Monte Carlo simulations [8] on a 2D Ising model demonstrate that the three observed plateaus of the ferrimagnetic phase are related to metastable magnetic states. On the other hand, X-ray absorption and magnetic circular dichroism reveal that there are anomalously large orbital moment of $1.7\mu_B$ along c -axis at the Co_{pri} sites [9]. This could be related to the very strong anisotropy with the moment preferentially aligned along c -axis induced by the crystalline electronic fields [2–4]. First-principles calculations [10] show the spin–orbit coupling and unusual coordination of the trigonal Co ion lead to the occupation of the d_{z^2} spin-down orbital, generating a giant orbital moment ($1.57\mu_B$). Very recently, $\text{Ca}_3\text{Co}_2\text{O}_6$ has also been found to exhibit a magnetodielectric effect below $T_N = 25$ K with a peak in the $\varepsilon(H)$ curve at the ferri to ferromagnetic transition [11].

The $\text{Ca}_3\text{Co}_2\text{O}_6$ crystal is composed of alternating CoO_6 trigonal prisms (Co_{pri}) and CoO_6 octahedra (Co_{oct}) running along the

c -axis of the hexagonal cell [1] with Ca ions separating these CoO_6 chains (Fig. 1). The hopping conductivity shows insulating behavior with an energy gap opened by the correlated d electrons [12]. NMR measurement [13], X-ray photoemission spectroscopy [14], and X-ray absorption [9] illustrate that both the Co_{pri} and Co_{oct} are trivalent. The Co_{oct} site is in a low-spin state with magnetic moment of $0.08\mu_B$, whereas Co_{pri} site is in the high-spin state with magnetic moment of $\sim 3\mu_B$ [1,9,13,14]. The intrachain and interchain couplings are ferromagnetic (FM) and antiferromagnetic (AFM), respectively [15,16]. The long Co–Co interchain distance (~ 5.3 Å), as compared to the short Co_{pri} – Co_{oct} intrachain distance (~ 2.6 Å), ensures the hierarchy of the magnetic exchange energies, $J_{intra} \gg J_{inter}$ [4].

In this work we investigate the electronic structure of $\text{Ca}_3\text{Co}_2\text{O}_6$ from first-principles. We find $\text{Ca}_3\text{Co}_2\text{O}_6$ a Mott–Hubbard insulator in the interchain ferrimagnetic ground state with a $3z^2 - r^2$ orbital ordering on the Co_{pri} sublattice driving the intrachain ferromagnetic coupling along c -axis.

2. Computational details

The electronic structures of $\text{Ca}_3\text{Co}_2\text{O}_6$ are calculated using the full-potential projected augmented wave method [17] as implemented in the VASP [18] package within the generalized gradient approximation (GGA) [19] and GGA plus Hubbard U (GGA + U) [20] scheme. The low-T ferrimagnetic rhombohedral $R\bar{3}c$ structure with 66 atoms per unit cell (Fig. 1) is used. The calculations were performed over a $5 \times 5 \times 5$ Monkhorst–Pack k -points grid in the irreducible Brillouin zone with cut-off energy of 500 eV. Coulomb energy $U = 5$ eV [10] and exchange parameter $J = 0.8$ eV are used for all Co ions.

* Corresponding authors.

E-mail addresses: g943318@phys.nthu.edu.tw (T.-R. Chang),

jeng@phys.sinica.edu.tw (H.-T. Jeng).

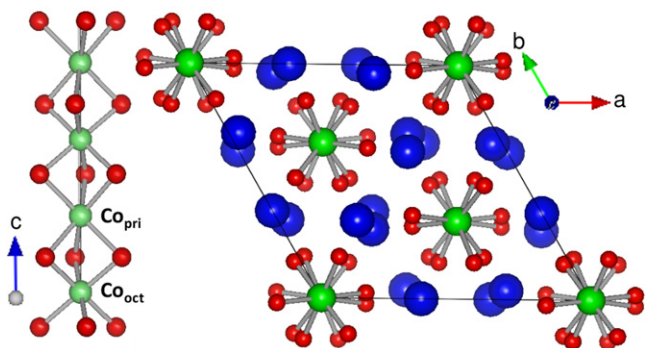


Fig. 1. Crystal structure of $\text{Ca}_3\text{Co}_2\text{O}_6$. Blue, green, and red spheres denote Ca, Co, and O atoms, respectively.

3. Result and discussion

Fig. 2(a) shows the GGA total density of states (DOS) of $\text{Ca}_3\text{Co}_2\text{O}_6$ in the ferrimagnetic (FI) phase, in which the spin of all the intrachain Co ions align ferromagnetically while the magnetization of one of the three CoO_6 chains are antiparallel to that of the other two chains. The Co 3d states dominate the energy band from E_F to -1.5 eV, while the O 2p states are of lower energy. The projected DOS of Co_{oct} and Co_{pri} ions in one CoO_6 chain are also plotted. It can be seen that both the Co_{oct} and Co_{pri} ions show half-metallic behaviors that only spin down electrons are conductive. Combined with contributions from the other ferro- and antiferro-magnetic chains, GGA gives a metallic ground state for the FI phase (Fig. 2(a)). We have also calculated the total energy of the ferromagnetic (FM) state. The resultant FM energy is 10 meV per unit cell lower than the FI one as listed in Table 1. Unfortunately both conclusions from GGA as discussed above are inconsistent with the experimental insulating FI ground state of $\text{Ca}_3\text{Co}_2\text{O}_6$ [15,16].

To verify if the strong correlation is responsible for these discrepancies, we perform GGA + U calculations for both the FI and FM states. As shown in Table 1, the total energy of FI state is 28 meV per unit cell lower than FM states from GGA + U , indicating a FI ground state of $\text{Ca}_3\text{Co}_2\text{O}_6$. Meanwhile the on-site Coulomb repulsion U opens up an energy gap (0.64 eV) at Fermi level as depicted in Fig. 2(b), leading $\text{Ca}_3\text{Co}_2\text{O}_6$ to a Mott insulator. Band structures calculations (not shown here) demonstrate that band dispersions are relatively strong along c -direction than over ab -plane, reflecting the structural quasi-one-dimensional character. The strong intrachain and weak interchain interactions implied by band dispersions also consist with hopping conductivity measurements [12].

The integrated Co valence charge and spin over atomic sphere of radius 1.0 Å are listed in Table 1. There exist slight charge separation of $\sim 0.1e$ between Co_{oct} and Co_{pri} ions from both GGA and GGA + U . Whereas the spin moments are very different for these two sites. The octahedral Co is nearly nonmagnetic while the prismatic Co is in the high spin state of $\sim 3\mu_B/\text{Co}$. To identify the energy levels, we project the Co d bands onto the five cubic harmonics as depicted in Fig. 3. From GGA, the Co_{pri} spin up channel is fully occupied, while in the spin down channel, the $3z^2 - r^2/x^2 - y^2/xy$ orbitals are partially occupied with the yz/zx orbitals empty. In contrast, the on-site U strongly localizes the spin up doubly degenerated $x^2 - y^2/xy$ and yz/zx bands and drastically lowers the band energy to -6.4 eV and -6.8 eV, respectively. While the spin down counterparts are pushed up above E_f , resulting in the ($d^5 \uparrow$, $d_{z^2}^1 \downarrow$) high spin state with nominal $4\mu_B/\text{Co}_{\text{pri}}$ and numerical and experimental $\sim 3\mu_B/\text{Co}_{\text{pri}}$. Since $3z^2 - r^2$ orbital (a_{1g} in the hexagonal symmetry) of both spin are fully occupied, the magnetic moment at Co_{pri} sites mainly comes from

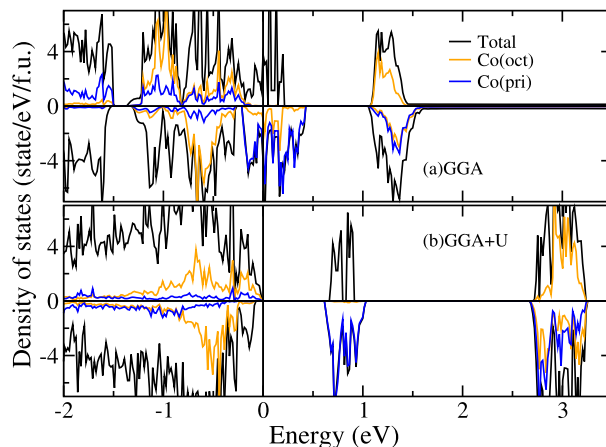


Fig. 2. DOS of $\text{Ca}_3\text{Co}_2\text{O}_6$ from GGA (a) and GGA + U (b). Black, red, and blue lines denote total, Co_{oct} , and Co_{pri} DOS, respectively. The Fermi level is at zero energy.

Table 1

Magnetic stability ($\Delta E = E_{\text{FI}} - E_{\text{FM}}$, meV/unit cell), energy gap (eV), valence charge (e), and magnetic moment (μ_B) of Co ions within atomic spheres of radius 1.0 Å in ferrimagnetic $\text{Ca}_3\text{Co}_2\text{O}_6$.

	ΔE	Gap	$\text{Co}_{\text{oct}}^{\text{charge}}$	$\text{Co}_{\text{pri}}^{\text{charge}}$	$\text{Co}_{\text{oct}}^{\text{spin}}$	$\text{Co}_{\text{pri}}^{\text{spin}}$
GGA	10	0	6.21	6.31	0.33	2.68
GGA + U	-28	0.64	6.51	6.40	0.01	2.92

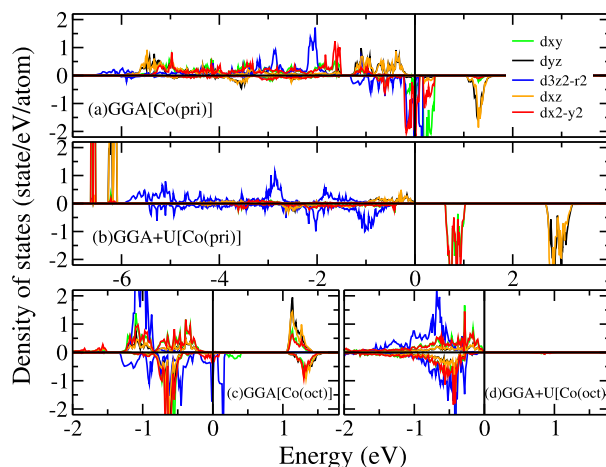


Fig. 3. DOS of $\text{Ca}_3\text{Co}_2\text{O}_6$ projected onto the 3d cubic harmonics from GGA (a) and GGA + U (b).

the low-energy $x^2 - y^2/xy$ and yz/zx orbitals (e'_g in the hexagonal symmetry). As for the Co_{oct} ions (Fig. 3(c, d)), both GGA and GGA + U gives approximately ($e'_g \uparrow a_{1g}^1 \uparrow$, $e'_g \downarrow a_{1g}^1 \downarrow$) low spin configuration in the hexagonal symmetry with a nearly zero moment. From the above energy level analysis, although there exists numerically slight charge disproportion, however both the Co_{oct} and Co_{pri} are nominally trivalent with 6 valence electrons. This result is support by experiments [9,13,14].

The Co_{pri} ($d^5 \uparrow$, $d_{z^2}^1 \downarrow$) and Co_{oct} ($e'_g \uparrow a_{1g}^1 \uparrow$, $e'_g \downarrow a_{1g}^1 \downarrow$) valence configurations from GGA + U discussed above and presented in Fig. 3 actually indicate the formation of $3z^2 - r^2$ orbital ordering on Co_{pri} sublattice. Fig. 4 shows the equal charge density surface in the energy interval (-1.5 eV $\sim E_f$) from GGA + U . At Co_{oct} site, the ellipsoid-like charge contour results from the fully occupied spin up and spin down e'_g and a_{1g} orbitals. While at Co_{pri} sites, the

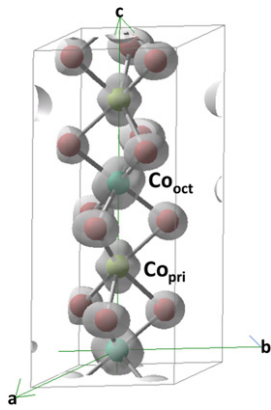


Fig. 4. Orbital ordering of $\text{Ca}_3\text{Co}_2\text{O}_6$. For clarity, only one CoO_6 chain is shown.

trigonal prism crystal field favors the a_{1g} ($3z^2 - r^2$) orbital. Hence both the spin up and spin down a_{1g} orbitals are fully occupied while e'_g is occupied by spin up electrons only (Fig. 3), forming the $3z^2 - r^2$ orbital ordering as shown in Fig. 4. We have also performed calculations using different values of U . Our results reveal that the energy gap at E_f and orbital ordering exists with U from 3 to 8 eV.

The relatively short intrachain bond distance of 2.6 Å between Co_{oct} and Co_{pri} leads to a direct overlap of $3z^2 - r^2$ orbitals of these two sites. As a result, the intrachain FM coupling between Co_{pri} ions would be induced by the indirect exchange interaction between the localized spin moments of Co_{pri} $x^2 - y^2/xy$ and yz/zx electrons (Fig. 3(b)) mediated by the relatively itinerant one-dimensional $3z^2 - r^2$ bands along c -axis. Our results are compatible with the argument that the $\text{Co}_{\text{oct}} - \text{Co}_{\text{pri}}$ distance is short enough for formation of an itinerant $3z^2 - r^2$ one-dimensional band [7] with ferromagnetic coupling [21]. The calculated total energy of the intrachain FM state is 23 meV per unit cell lower than the intrachain AFM state. We note this is close to the corresponding interchain value of 28 meV (Table 1), indicating that J_{intra} is similar to J_{inter} in spite of the chain structure. This could be understood by the following two reasons: First, the nonmagnetic Co_{oct} ion strongly screens the magnetic interactions between two Co_{pri} ions. Second, the distance between two Co_{pri} ions is about 5.2 Å, which is nearly equal to the inter-chain distance of ~ 5.3 Å. Nevertheless the intrachain electronic interaction is certainly stronger than the interchain one, leading to the stronger band dispersions along the c -axis as mentioned previously.

4. Conclusion

We have investigated the electronic structures of $\text{Ca}_3\text{Co}_2\text{O}_6$ using GGA and GGA + U formalisms. We found $\text{Ca}_3\text{Co}_2\text{O}_6$ is a FI

Mott insulator rather than a FM metal. In addition, we found an associated $3z^2 - r^2$ orbital ordering on Co_{pri} sublattice induced by on-site U . This $3z^2 - r^2$ orbital ordering plays important role in forming the intrachain FM ground state. Our finding suggests that strong electron–electron correlation is important in quasi-one-dimensional $\text{Ca}_3\text{Co}_2\text{O}_6$.

Acknowledgements

This work was supported by the National Science Council of Taiwan and Academia Sinica.

We also thank NCHC, CINC-NTU, and NCTS for technical supports.

References

- [1] S. Aasland, H. Fjellvag, B. Hauback, Solid State Commun. 101 (1997) 187.
- [2] H. Kageyama, K. Yoshimura, K. Kosuge, H. Mitamura, T. Goto, J. Phys. Soc. Jpn. 66 (1997) 1607.
- [3] H. Kageyama, K. Yoshimura, K. Kosuge, M. Azuma, M. Takano, H. Mitamura, T. Goto, J. Phys. Soc. Jpn. 66 (1997) 3996.
- [4] A. Maignan, C. Michel, A.C. Masset, C. Martin, B. Raveau, Eur. Phys. J. B 15 (2000) 657.
- [5] J.-G. Cheng, J.-S. Zhou, J.B. Goodenough, Phys. Rev. B 79 (2009) 184414.
- [6] D. Flahaut, A. Maignan, S. Hebert, C. Martin, R. Retoux, V. Hardy, Phys. Rev. B 70 (2004) 094418.
- [7] V. Hardy, M.R. Lees, O.A. Petrenko, D.McK. Paul, D. Flahaut, S. Hebert, A. Maignan, Phys. Rev. B 70 (2004) 064424.
- [8] R. Soto, G. Martínez, M.N. Baibich, J.M. Florez, P. Vargas, Phys. Rev. B 79 (2009) 184422.
- [9] T. Burnus, Z. Hu, M.W. Haverkort, J.C. Cezar, D. Flahaut, V. Hardy, A. Maignan, N.B. Brookes, A. Tanaka, H.H. Hsieh, H.-J. Lin, C.T. Chen, L.H. Tjeng, Phys. Rev. B 74 (2006) 245111.
- [10] Hua Wu, M.W. Haverkort, Z. Hu, D.I. Khomskii, L.H. Tjeng, Phys. Rev. Lett. 95 (2005) 186401.
- [11] Natalia Bellido, Charles Simon, Antoine Maignan, Phys. Rev. B 77 (2008) 054430.
- [12] B. Raquet, M.N. Baibich, J.M. Broto, H. Rakoto, S. Lambert, A. Maignan, Phys. Rev. B 65 (2002) 104442.
- [13] E.-V. Sampathkumaran, N. Fujiwara, S. Rayaprol, P.K. Madhu, Y. Uwatoko, Phys. Rev. B 70 (2004) 014437.
- [14] K. Takubo, T. Mizokawa, S. Hirata, J.-Y. Son, A. Fujimori, D. Topwal, D.D. Sarma, S. Rayaprol, E.-V. Sampathkumaran, Phys. Rev. B 71 (2005) 073406.
- [15] V. Hardy, S. Lambert, M.R. Lees, D.McK. Paul, Phys. Rev. B 68 (2003) 014424.
- [16] V. Hardy, M.R. Lees, A. Maignan, S. Hebert, D. Flahaut, C. Martin, D.McK. Paul, J. Phys.: Condens. Matter 15 (2003) 5737.
- [17] P.E. Blöchl, Phys. Rev. B 50 (1994) 17953; G. Kresse, J. Joubert, Phys. Rev. B 59 (1999) 1758.
- [18] G. Kress, J. Hafner, Phys. Rev. B 48 (1993) 13115; G. Kress, J. Furthmüller, Comput. Mater. Sci. 6 (1996) 15; G. Kress, J. Furthmüller, Phys. Rev. B 54 (1996) 11169.
- [19] J.P. Perdew, K. Burke, M. Ernzerhof, Phys. Rev. Lett. 77 (1996) 3865.
- [20] A.I. Liechtenstein, V.I. Anisimov, J. Zaanen, Phys. Rev. B 52 (1995) R5467.
- [21] J.B. Goodenough, Magnetism and the Chemical Bond, Interscience, Wiley, New York, 1963; R. Frésard, C. Laschinger, T. Kopp, V. Eyert, Phys. Rev. B 69 (2004) 140405(R).